

Supporting Information

Alloy/strain engineering of Pt-based nanowires with controllable electronic structure towards boosted water electrolysis catalysis

Jiakang Tian,^{†a,d} Senmin Lin,^{†b} Zhongmin Tang,^{†b} Runhua Li,^{a,d} Xiaomei Cheng,^b Zhen Fang,^{a,d} Bin Wang,^b Jiaheng Peng,^{*a,d} Lang Xiao,^b Benwei Fu,^a Tao Deng,^{*a,c} and Jianbo Wu^{*a,b,c,d}

^a State Key Laboratory of Metal Matrix Composites, School of Materials Science and Engineering, Shanghai Jiao Tong University, Shanghai 200240, P. R. China. E-mail: jianbowu@sjtu.edu.cn

^b Emergency Rescue Center of Xinjiang Oilfield Company

^c Center of Hydrogen Science, Shanghai Jiao Tong University, Shanghai 200240, P. R. China.

^d Future Material Innovation Center, Zhangjiang Institute for Advanced Study, Shanghai Jiao Tong University, Shanghai 200240, P. R. China.

* Corresponding Author

E-mail: pengjiaheng_2016@sjtu.edu.cn (J. Peng); dengtao@sjtu.edu.cn (T. Deng); jianbowu@sjtu.edu.cn (J. Wu)

[†] These authors contributed equally to this paper.

Methods

Chemicals: Potassium tetrachloroplatinate (K_2PtCl_6 , $\geq 99.0\%$), iridium acetylacetonate ($Ir(acac)_3$, $\geq 97.0\%$), and ruthenium acetylacetonate ($Ru(acac)_3$, $\geq 97.0\%$) was purchased from Aladdin. Deionized water (DI water) used was $18.2 M\Omega$ cm. Anhydrous ethanol (EtOH, AR, $\geq 99.7\%$) and isopropanol (C_3H_8O , AR, $\geq 99.7\%$) were purchased from

Sinopharm Chemical Reagent Co.,Ltd. Commercial Pt/C (HP 20 wt.% Pt) was purchased from Alfa Aesar. Amorphous carbon (C, Vulcan® XC-72R) purchased from Cabot were used as support materials. The H₂/Ar (5%/95%) gas was purchased from Shanghai Weichuang Standard Gas Analytical Technology Co., Ltd. All the chemicals and materials were used as received.

Synthesis of Pt-300 NWs: For the typical synthesis of free-standing Pt NWs, 38.6 mg K₂PtCl₄ was thermally treated in a vacuum oven at 60 °C to remove the moisture prior to be paved onto the quartz boat so that the precursors could have full access to the reducing gas then transferred into the reactor. The H₂/Ar (5%/95%) gas was injected after the whole system had been purged. The dried Pt precursors were then reduced by being heated for 28 min to 300 °C and maintained at the temperature for 30 min. The samples were washed with deionized water to remove the unreduced metal precursors, then subsequently underwent centrifugation at 6000 rpm for once, then dispersed the free-standing Pt NWs in ethanol before any characterization and test in case of segregation. No further washing process was used.

Synthesis of PtRu-300 NWs: For the typical synthesis of free-standing PtRu NWs, 38.6 mg K₂PtCl₄ and 8.2 mg Ru(acac)₃ were mixed and thermally treated in a vacuum oven at 60 °C to remove the moisture prior to be paved onto the quartz boat so that the precursors could have full access to the reducing gas then transferred into the reactor. The H₂/Ar (5%/95%) gas was injected after the whole system had been purged. The dried Pt precursors were then reduced by being heated for 28 min to 300 °C and maintained at the temperature for 30 min. The samples were washed with deionized water to remove the unreduced metal precursors, then underwent centrifugation at 6000 rpm for once, then dispersed the free-standing Pt NWs in ethanol before any characterization and test in case of segregation. No further washing process was used.

Synthesis of PtIr NWs: For the typical synthesis of free-standing PtRu NWs, 38.6 mg K₂PtCl₄ and 10.1 mg Ir(acac)₃ were mixed and thermally treated in a vacuum oven at

60 °C to remove the moisture prior to be paved onto the quartz boat so that the precursors could have full access to the reducing gas then transferred into the reactor. The H₂/Ar (5%/95%) gas was injected after the whole system had been purged. The dried Pt precursors were then reduced by being heated for 28 min to 300 °C and maintained at the temperature for 30 min to obtain the PtIr-300 NWs. The samples were washed with deionized water to remove the unreduced metal precursors, then subsequently underwent centrifugation at 6000 rpm for once, then dispersed the free-standing Pt NWs in ethanol before any characterization and test in case of segregation. No further washing process was used. The temperature-dependent control experiments were conducted with the same synthesis process for free-standing PtIr NWs. The precursors were reduced by being heated to 250 °C, 350 °C and 400 °C with a rate of 10 °C min⁻¹ and maintained at the temperature for 30 min to obtain the PtIr-250 NWs, PtIr-350 NWs, and PtIr-400 NWs, respectively.

Materials Characterization: Transmission electron microscopy (TEM) images, the energy-dispersive X-ray spectra (EDX), the high-resolution TEM (HRTEM), high-angle annular dark-field scanning transmission electron microscopy (HAADF-STEM), and energy-dispersive X-ray spectroscopy (EDS) mapping were performed on Talos F200X G2 operated at 200 kV. All the TEM samples were prepared by dropping 6 μL n-hexane or ethanol dispersion of samples onto carbon film-coated copper grids with pipettes and dried under ambient conditions. Powder X-ray diffraction (PXRD) patterns were recorded on a Rigaku Smart Lab operating at 30 mA and 40 kV with a Cu K α X-ray source ($\lambda=1.5418$ Å). X-ray photoelectron spectroscopy (XPS) analysis was conducted on the Thermo Fisher Scientific K-alpha+ with monochromatic Al k- α (1486.68 eV) source. All binding energies were calibrated to C 1s adventitious carbon at 284.8 eV.

Electrochemical measurements:

Electrochemical tests were carried out on an electrochemical workstation (CHI 760E). A typical three-electrode system was used with a glass carbon rotating disk electrode (RDE, diameter: 5 mm, area: 0.196 cm⁻²) as the working electrode, a platinum mesh (1

cm⁻²) or a graphite rod as the counter electrode, and an Ag/AgCl as the reference electrode. The RDE was carefully S4 polished and cleaned several times before each experiment. Subsequently, 6.0 μ L of the ink was dropped on an RDE to form a smooth thin film. The mass loading of the catalyst was 15.3 μ g \cdot cm⁻².

Linear sweep voltammograms (LSV) polarization curves were collected in both 1.0 M. KOH and 0.5 M H₂SO₄ at the potential scanning rate of 5 mV s⁻¹ and 95% iR compensation. The scanning potentials were from -0.2 to 0.2 V for HER.

All the potentials referred to the Ag/AgCl or SCE were converted to the reversible hydrogen electrode using the Nernst equation.

$$E(\text{RHE}) = E(\text{SCE}) + 0.241 + 0.0591 \times \text{pH} \quad (1)$$

$$E(\text{RHE}) = E(\text{Hg}/\text{HgO}) + 0.098 + 0.0591 \times \text{pH} \quad (2)$$

$$E(\text{RHE}) = E(\text{Ag}/\text{AgCl}) + 0.199 + 0.0591 \times \text{pH} \quad (3)$$

Overpotential Calculations:

The HER overpotential (η) was calculated according to the following formula:

$$\eta \text{ (V)} = -E(\text{RHE}) \quad (4)$$

the OER overpotential (η) was calculated according to the following formula:

$$\eta \text{ (V)} = E(\text{RHE}) - 1.23 \quad (5)$$

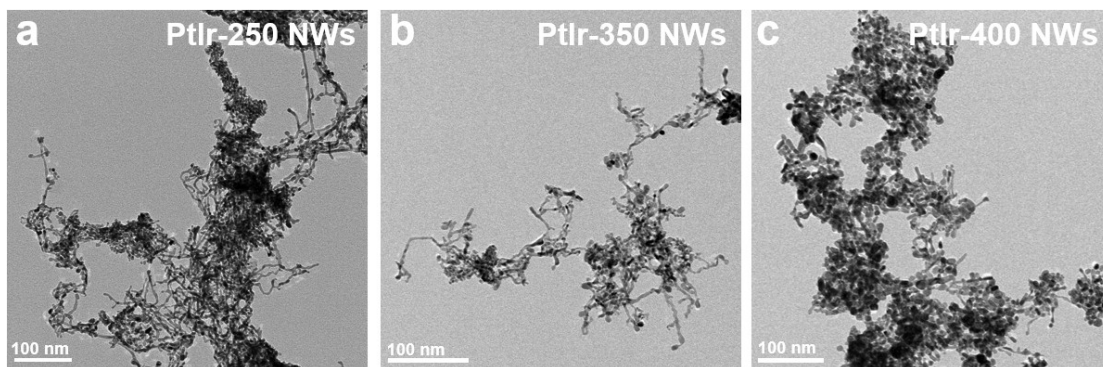


Fig S1. Low-magnification TEM image of a) PtIr-250 NWs, b) PtIr-350 NWs, and c) PtIr-400 NWs.

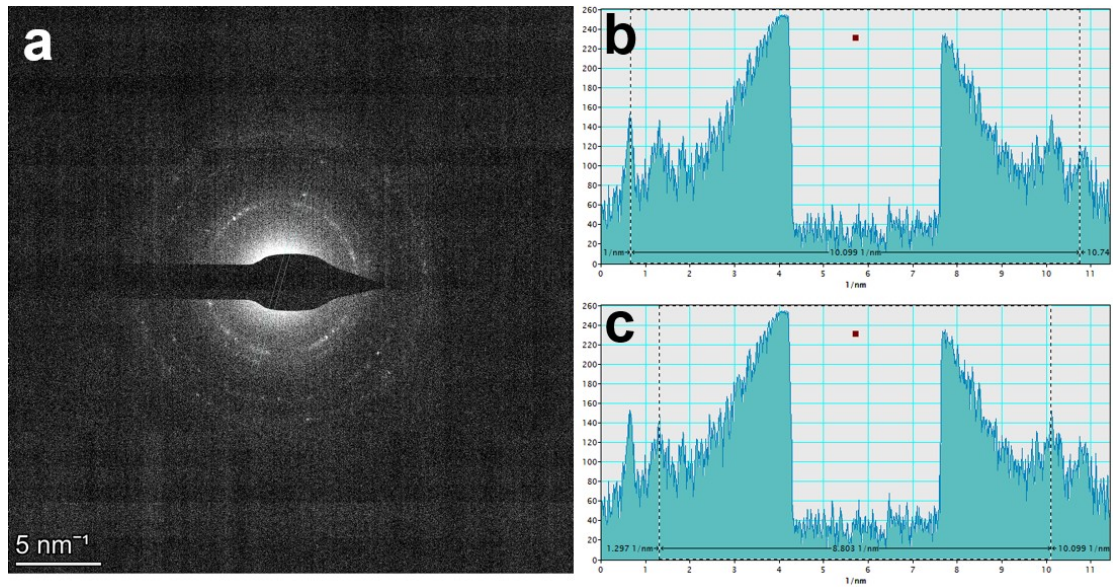


Fig S2. a) The corresponding SAED image of PtIr-350 NWs. The integrated pixel intensities in b) PtIr(200) facets and c) PtIr(111) facets.

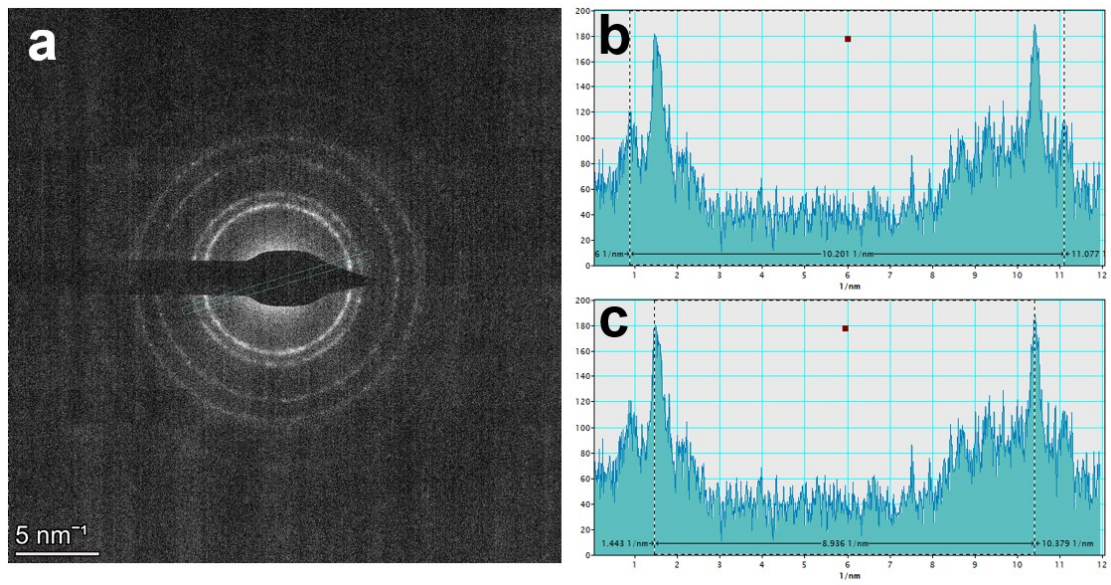


Fig S3. a) The corresponding SAED image of PtIr-250 NWs. The integrated pixel intensities in b) PtIr(200) facets and c) PtIr(111) facets.

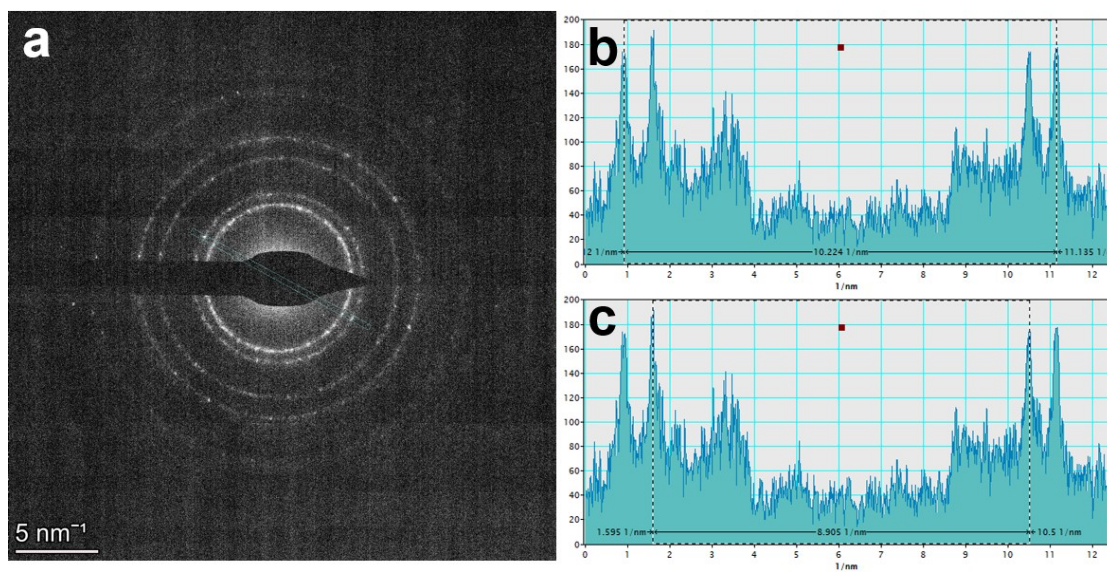


Fig S4. a) The corresponding SAED image of PtIr-400 NWs. The integrated pixel intensities in b) PtIr(200) facets and c) PtIr(111) facets.

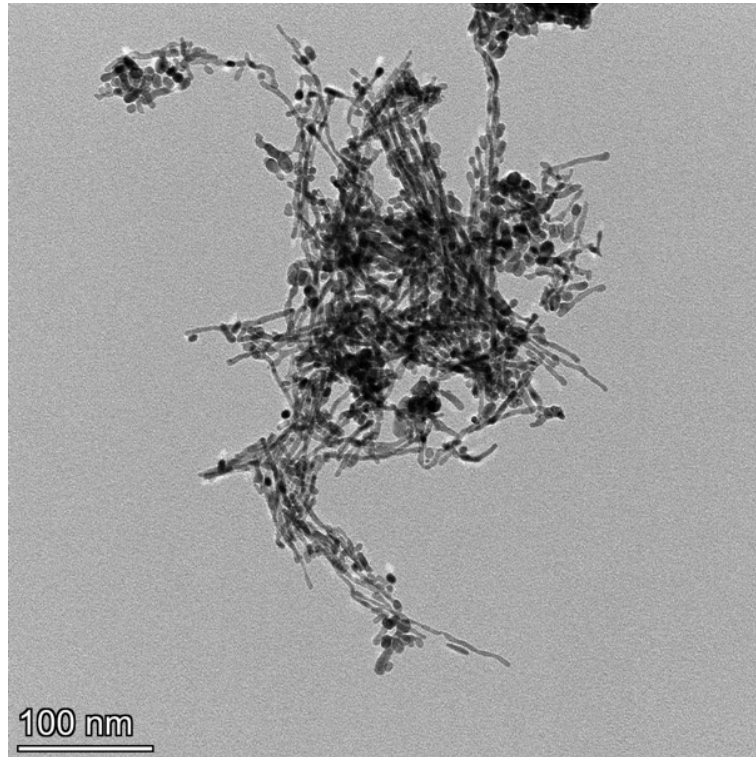


Fig S5. Low-magnification TEM image of Pt-300 NWs.

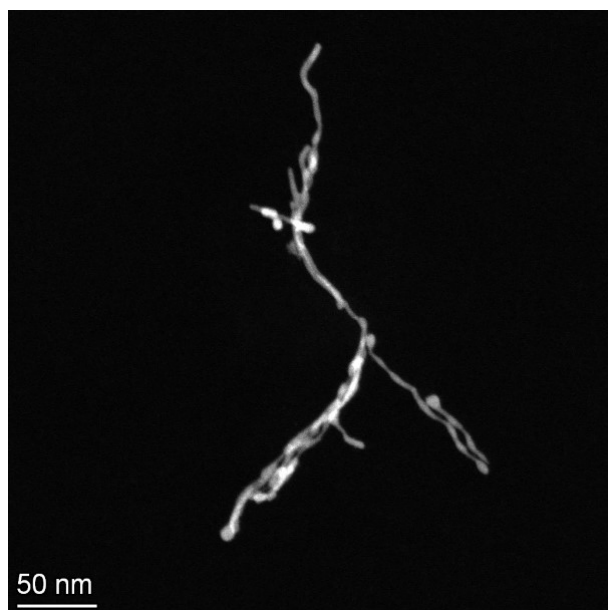


Fig S6. Low-magnification HADDF-STEM image of PtRu-300 NWs.

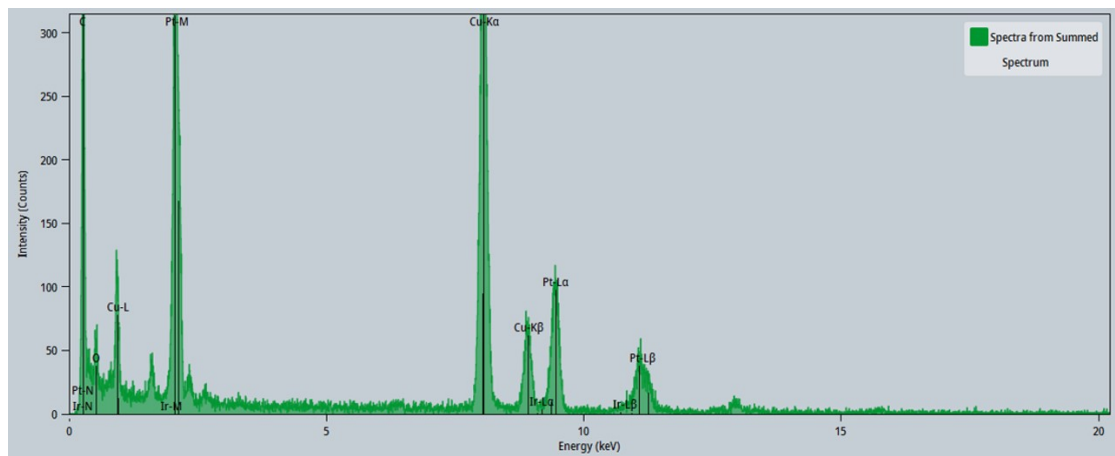


Fig S7. EDX spectrum of PtIr-250 NWs.

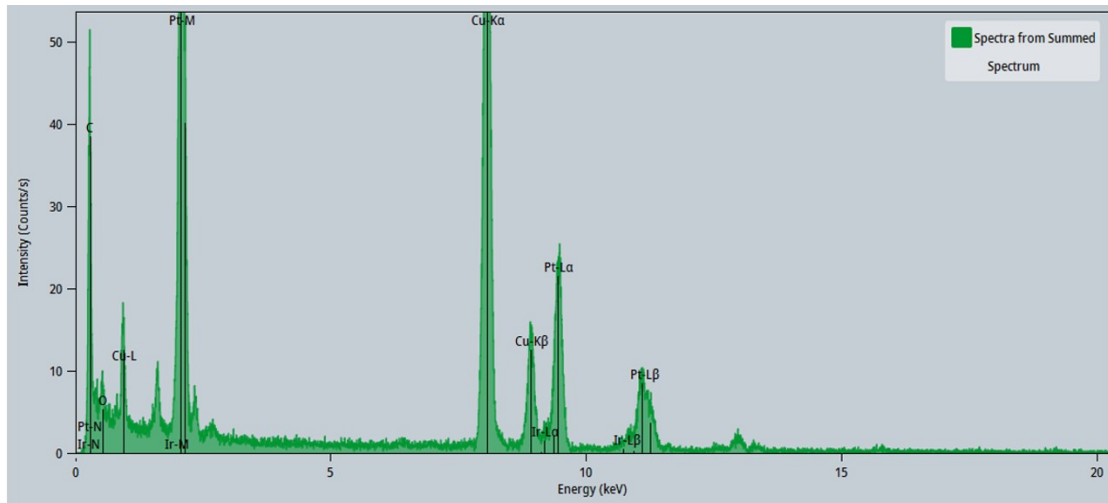


Fig S8. EDX spectrum of PtIr-300 NWs.

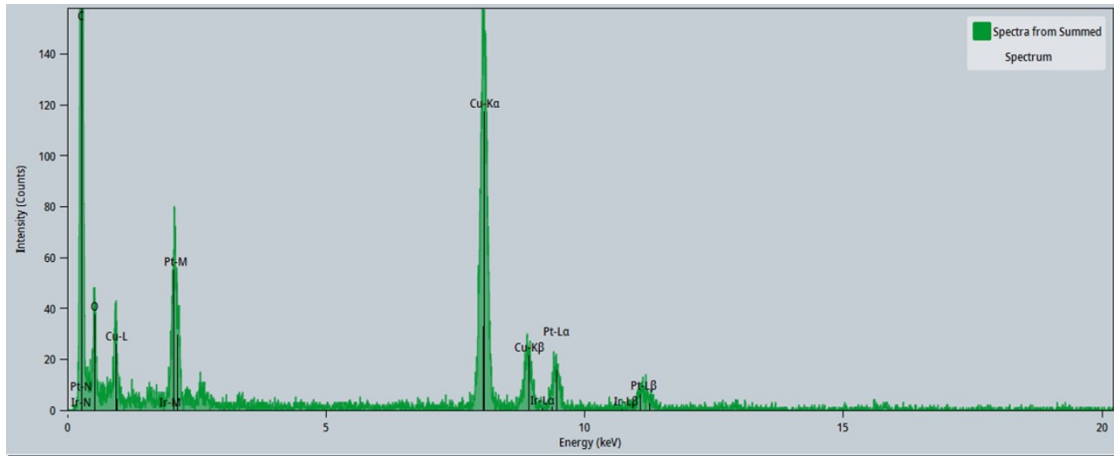


Fig S9. EDX spectrum of PtIr-350 NWs.

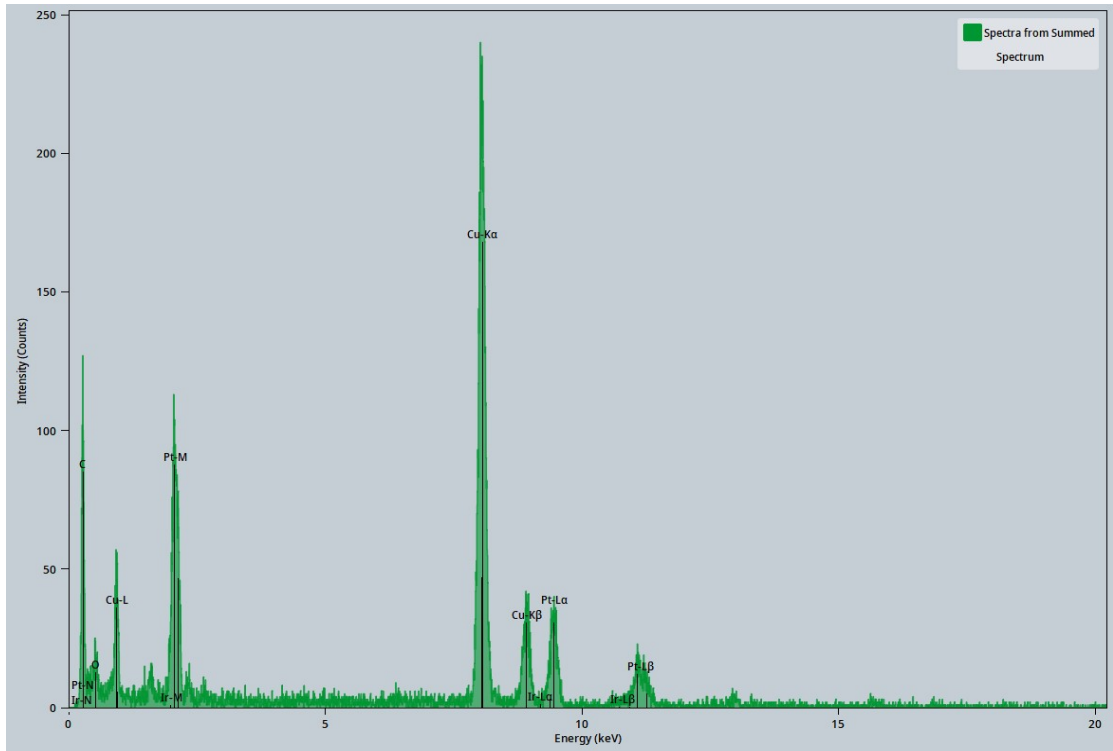


Fig S10. EDX spectrum of PtIr-400 NWs.

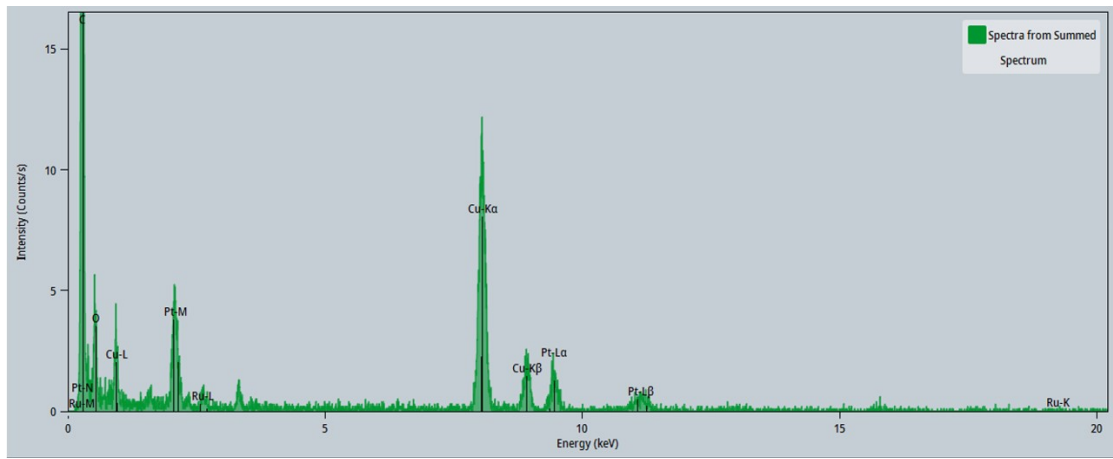


Fig S11. EDX spectrum of PtRu-300 NWs.

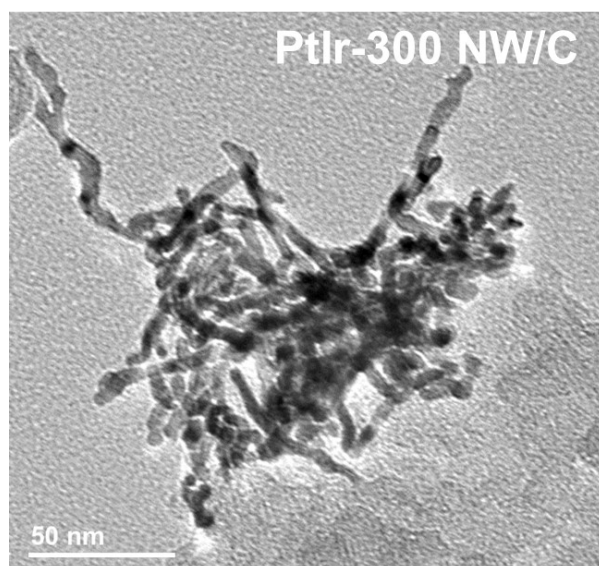


Fig S12. Low-magnification TEM image of Pt-300 NWs/C after i-t test for 24 h.

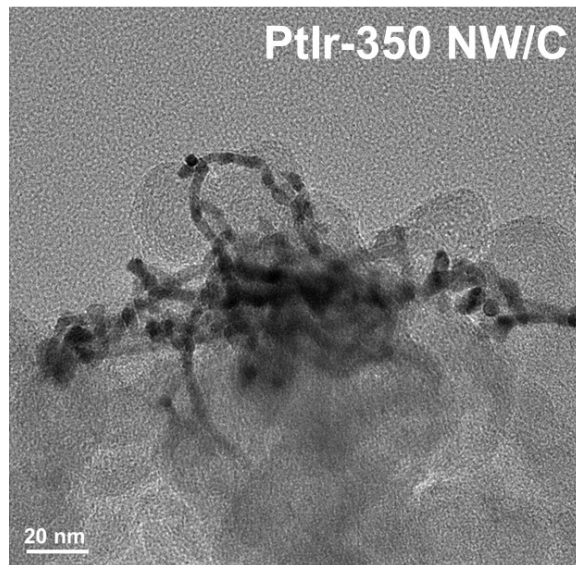


Fig S13. Low-magnification TEM image of Pt-350 NWs/C after i-t test for 24 h.

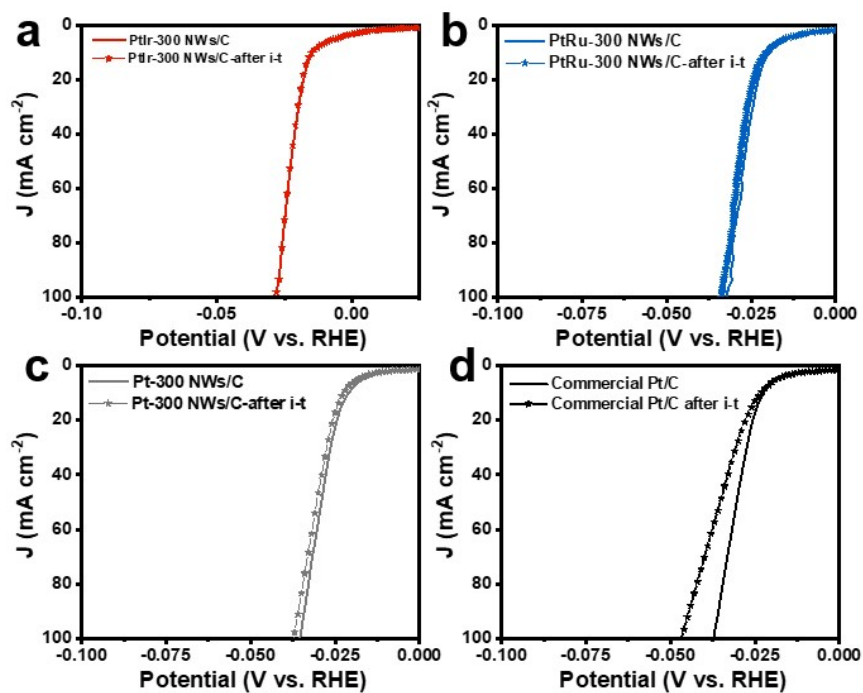


Fig S14. HER polarization curves of a) PtIr-300 NWs/C, b) PtRu-300 NWs/C, c) Pt-300 NWs/C, and d) commercial Pt/C catalysts recorded before and after the i-t test.

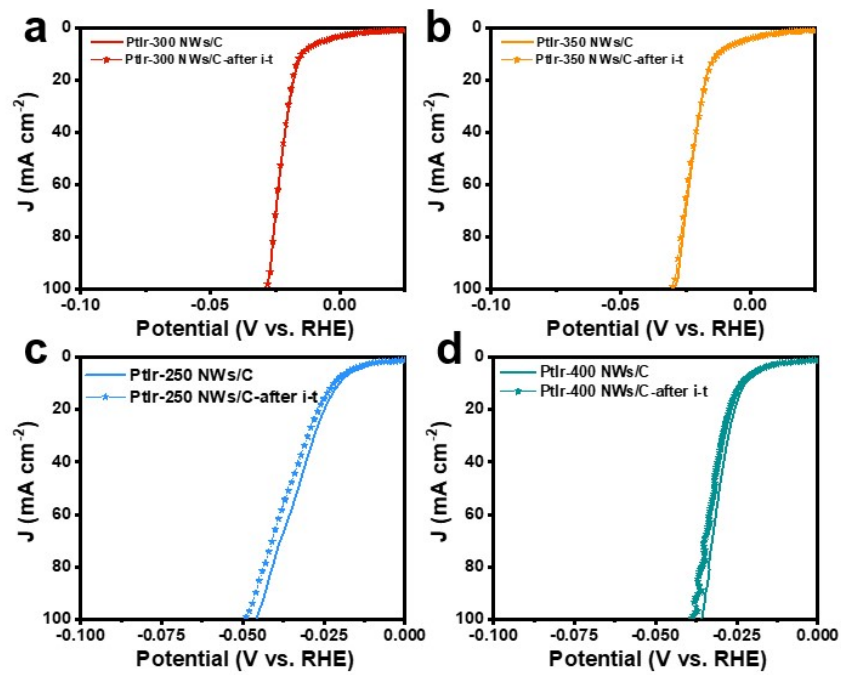


Fig S15. HER polarization curves of a) PtIr-300 NWs/C, b) PtIr-350 NWs/C, c) PtIr-250 NWs/C, and d) PtIr-400 NWs/C catalysts recorded before and after i-t test.

Table S1 Comparison of elemental quantification for the catalysts in this work.

Sample	Pt atom%	Ir (Ru) atom%
PtIr-250 NWs/C	84.61	15.39
PtIr-300 NWs/C	83.43	16.57
PtIr-350 NWs/C	85.23	14.77
PtIr-400 NWs/C	82.35	17.65
PtRu-300 NWs/C	85.90	14.10

Table S2. Comparison of HER performance for the catalysts in this work.

Sample	$\eta@10$ and 100 mA cm^{-2} (mV)	Tafel slope (mV dec^{-1})	$\eta@10$ and 100 mA cm^{-2} (mV, after i-t test)	Mass activity@10 and 15 mV ($\text{A mg}_{\text{PGM}}^{-1}$)	ECSA ($\text{m}^2 \text{g}_{\text{PGM}}^{-1}$)	Intrinsic activity@10 and 15 mV (mA cm^{-2})
PtIr-300 NWs/C	9/18	10.0	9/20	0.25/1.14	23.19	1.07/4.93
PtRu-300 NWs/C	19/32	13.6	20/34	0.07/0.11	11.97	0.55/0.91
PtIr-350 NWs/C	14/28	12.1	14/30	0.13/0.21	17.48	0.74/1.20
PtIr-250 NWs/C	20/46	21.7	22/49	0.05/0.09	8.06	0.67/1.15
PtIr-400 NWs/C	22/35	14.5	23/38	0.05/0.07	7.18	0.66/0.99
Pt-300 NWs/C	21/35	13.0	23/38	0.05/0.08	9.32	0.53/0.86
Commercial Pt/C	23/47	16.7	22/50	0.05/0.07	66.71	0.07/0.10